The trembling hand unraveled: the motor dynamics and neural sources of choice inconsistency

Vered Kurtz-David[1,2*], Asaf Madar[3#], Adam Hakim[3#], Noa Palmon[3] & Dino J Levy[1,3]

[1] Coller School of Management, Tel Aviv University, Tel Aviv, Israel

[2] Grossman School of Medicine, New York University, New York, USA

[3] Sagol School of Neuroscience, Tel Aviv University, Tel Aviv, Israel

(*) Corresponding author: Vered Kurtz-David at kurtzv02@nyu.edu

(#) Equal second-author contribution

Abstract

Ample evidence shows that humans violate fundamental economic axioms. Yet, the neural mechanism underlying inconsistent (or irrational) choices remains obscure. Here, we aim to show that inconsistent choices could rise either due to value miscalculations or due to motor errors during task execution. We report the results from two independent behavioral and neuroimaging studies. Subjects completed a risky-choice task to test their inconsistency levels, followed by two novel tasks, designed to solely examine motor output. We recorded mouse trajectories during task execution and designed 34 features to analyze choice dynamics. We show that choice dynamics predict inconsistency levels, even when motor output was absent any valuation elements. In the neuroimaging study, we show that inconsistency is tied to noisy value computations in reward circuits, but at the same time, is also related to noisy neural motor dynamics. These findings suggest that (at least) two neural sources of noise contribute to inconsistent choice behavior.

Keywords

Value-based decision-making, mouse-tracking, fMRI, choice execution, motor cognition, irrational choice

Main text

Imagine you are in the arcade, trying to pull your favorite blue teddy bear out of the claw machine. However, for some reason, you end up grabbing a less preferred red teddy bear instead of the blue one. This inconsistency between your "true" preference and your actual choice can be the result of (at least) two different kinds of errors: it might be that you were confused about the values of each teddy bear, leading to suboptimal inference[1,2]. It might also be that you accurately calculated the "correct" values of the options, but had a moment of motor "clumsiness", when you reached out to grab the doll.

In the 1970s, Nobel-prize laureate Reinhard Selten has coined the term "*trembling hand error*", referring to the possibility that decision makers choose suboptimal options with small probabilities[3]. This notion has become a synonym for accidental outcomes in decision-making. Nonetheless, as the term implies, and demonstrated in the arcade example, such mistakes could be the result of altered value representations, and/or due to motor tremor that accompanied choice execution.

Previous studies demonstrated how explore-exploit strategies[4,5] or recent reward history[6], can lead to stochastic decision-making and suboptimal value-based choices. Other scholars also argued for an additional source for these behaviors – random neural activity or noise[1,2,5,7–9]. However, most of these studies have focused on noise from sensory sources[10], as well as randomness which rises during the decision or valuation process in variable environments[11], sometimes referred to as inference noise[1]. At the same time, scholars argued that motor imprecision in task execution is a result of noise stemming from motor neural circuits[12,13]. A lot less is known on how motor noise, which is independent of inference or sensory noise, contributes to value-based decision making in general, and to inconsistency in choices in particular.

Choice inconsistency violates fundamental axioms in economic theory[14–16], as it disobeys the law of transitivity and creates choice cycles. Inconsistency nullifies the feasibility of the maximization of a utility construct[14], subjects choose irrationally, and hence, "leave money on the table"[17]. Importantly, choice inconsistency occurs even when the choice environment remains unchanged, absent any context manipulations induced by the experimenter[18–20]. As such, it resembles well-documented findings in perceptual and psychophysics studies that noisy random mechanisms vary perception and motor output, even when the stimuli, environment, or task remain constant[10]. This suggests that choice inconsistency may stem from noisy neural processes in various brain systems.

In the current work, we aim to differentiate between two sources of noise and argue that both sources contribute to choice inconsistency. The first source is related to neural activity in value-related brain areas (inference noise or value miscalculations), corresponding to a previous work from our lab[18]. The second source is related to noise in motor planning and execution processes that originates from motor-related brain regions. Demonstrating the contribution of motor-related noise to violations of economic theory, provides a more mechanistic neural-based approach to choice inconsistency than the general psychological and cognitive theories that dominate the literature[21].

To examine the possible sources of inconsistent choice, we use a well-studied task with a simple graphical interface[22] for eliciting subjects' inconsistency levels based on choices from linear budget sets[18–20,22,23]. Our task allows to estimate the overall level of inconsistency on the subject-level[19,23], as well as the severity of the inconsistency on a given trial[18]. Previous studies that used this task neglected the vast dynamic information concealed within the process of executing each choice. To this end, in addition to analyzing choice behavior, we also study the dynamics of the motor movements leading up to an inconsistent choice by analyzing mouse trajectories. Nevertheless, the greatest challenge when attempting to tease apart the two sources for suboptimality in choice, is to differentiate between motor errors in task execution from value miscalculations within the decision process per se. To overcome this, we present a novel task design, which solely captures motor output without any value computations. We then use the rich dynamic information of the mouse tracking data, to quantify the contribution of each of the two sources to the intensity of inconsistency levels.

Our work leverages the vast literature in recent years on mouse tracking tools, usually used in binary choice tasks, to investigate cognitive processes underlying subjects' behavior[24,25] in general, and value-based decision-making mechanisms in particular[26–28]. Importantly, not only does the mouse tracking data allow us to differentiate the sources for suboptimal choice, but it also enables us to identify the particular elements within the motor dynamics that contribute to inconsistent choice behavior. Finally, we employ neuroimaging techniques to examine the neural footprints of choice dynamics, and to pinpoint the different neural circuits related to the two sources that contribute to inconsistent choices.

We report the results from two separate studies: a behavioral study (n=89), and a neuroimaging study (n=42). Our main behavioral findings show that motor output, even when absent value modulation, predicts inconsistency levels, and thus, can be regarded as a source for suboptimality in choice. In the neuroimaging study, we replicated our previous findings, and show that inconsistent choice is related to noisy neural networks during the computation of value[18], but at the same time, we also demonstrate that inconsistency is strongly tied to the

neural dynamics in motor brain regions. Taken together, these findings suggest a substantial role of motor circuits in inconsistent choice. We show that 15- 20% of inconsistency reflects motor computational errors. This suggests a much greater role to motor output in suboptimal choice than reported in previous studies[1,5], perhaps due to the complexity of the motor demand induced by our design.

Results

Inconsistency and choice behavior

Subjects completed a risky choice task that allowed us to test their inconsistency levels[18,19] (Fig. 1a left panel, Methods and Supplementary Note 1). On each trial, subjects were facing a budget set with a varying slope and endowment, such that each bundle along the line is a 50-50% lottery between the X and Y amounts. Subjects used a mouse (behavioral study) or a trackball (neuroimaging study) to choose their most desired lottery, while their mouse trajectories were recorded.

Subjects had no difficulty understanding the task (Supplementary Fig. 1) and responded to changes in prices (slopes), following the Law of Demand (Fig. 2b). Based on subjects' choices in the risky choice task, we estimated their number of violations of the General Axiom of Revealed Preference (GARP)[14]. We report two different inconsistency measures for the intensity of violations: Afriat Index (AI)[17] and the Money Metric Index (MMI)[29] (Fig. 2a). Subjects in the behavioral study made on average more GARP violations compared to the sample in our previous study[18] ($p<0.0001$, two-tailed t-test), probably due to the higher number of trials subjects encountered (150 vs. 108, see Fisman et al., 2007)[20] (Fig. 2a, pink boxplots). Subjects in the neuroimaging study made a similar number of GARP violations compared to our previous fMRI study[18], ($p=0.231$, two-tailed t-test), and had similar inconsistency levels (AI: $p=0.196$, MMI: $p=0.970$, two-tailed t-test). However, they had fewer violations than subjects in the behavioral study ($p<0.0001$, two-tailed t-test), as well as lower inconsistency levels (AI: $p<0.0001$, MMI: $p=0.037$, two-tailed t-test), probably due to the lower number of trials (75 vs. 150)[20] (Fig. 2a, blue boxplots). Nonetheless, participants did not choose at random, as subjects in both studies exhibited substantially lower inconsistency levels compared with simulated random decision-makers[30] (all inconsistency measures, $p<0.0001$, one-tail t-test, Fig. 2a, yellow and green boxplots). Similarly to our previous study[18], for the trial-level analysis we focus on the trial-level-MMI index (henceforth: MMI, Methods and Supplementary Note 4).

[Insert Fig. 1 here]

[Insert Fig. 2 here]

Extracting motor related features

As a first step towards understanding motor output in our task, after analyzing subjects' submitted choices and measuring their level of choice inconsistency in each trial, we systematically examined and analyzed the motor dynamics leading up to a choice. Therefore, in both studies we recorded the mouse trajectories of motion pathways until the final choice was made (see Supplementary Note 5 and Supplementary Fig. 2 for descriptive results from the mouse tracking analysis). To take full advantage of the information concealed in the rich datasets provided by the mouse trajectories, we extracted various features from the mouse trajectories (see Methods and Supplementary Note 3 for details). Our aim was to characterize as many aspects of the motor dynamics as possible. We thus extracted a total of 34 different mouse features, such as the mean velocity of movement, layover time at the axes-origin, the aggregated curvature of the trajectory, time spent outside the axes-grid or the entropy of the trajectory pathway. See Fig. 3a-d for visualizations of four representative features, Supplementary Table 3 for a detailed list of all the features and Supplementary Figs. 3-4 for the distributions of features across the two studies. Fig. 3e illustrates the distribution across subjects of mouse features' values across trials (same features as in Fig. 3a-d), and suggests that there was high variability in response strategies within and across subjects. The variability in response strategies, even for similar choices (compare trajectories in the two panels of Supplementary Fig. 2b) is a first indication that motor circuits played a significant role in the decision process, one that could affect choice outcome and, accordingly, also affect inconsistency levels.

[Insert Fig. 3 here]

Choice dynamics predict inconsistency levels

Our main goal was to demonstrate that, in addition to value miscalculations (inference noise), choice inconsistency is influenced by the dynamics of motor charateristics originating in noisy neural computations in motor networks unrelated to value-based computations. Hence, we first wanted to show that motor dynamics, regardless of their cognitive or neural source, could

capture inconsistent choice behavior. Therefore, we aimed to relate the extracted mouse features from the value-based task to inconsistency scores on a subject-by-subject level.

Since the mouse features were highly correlated (Fig. 4a) and to avoid overfitting, we induced a dimensionality reduction procedure of the mouse features. We conducted a linear regression with elastic net regularization (see Methods) that resulted in a subset of mouse features out of the total 34 features. The advantage of using this approach is that it maintains the original mouse features, which allows interpretability of the results. Specifically, 15 (behavioral study) and 5 (neuroimaging study) features were selected by the elastic net regularization and significantly correlated with inconsistency levels ($p<0.05$, multiple linear model with subjects fixed effects, Fig. 4c, Supplementary Table 4, and Methods). This suggests that specific elements in task execution accounted for inconsistency levels. Goodness-of-fit measures show that task-execution mouse features accounted for 26.4% (behavioral study) and 18.3% (neuroimaging study) of the variance of inconsistency scores (Fig. 4d. See model equation in Methods). We further conducted a leave-one-subject-out prediction (see Methods). We found a positive correlation between predicted and actual inconsistency scores for all subjects in the behavioral study and for 39 of 42 subjects in the neuroimaging study ($p<0.0001$, one-sided t-test, median correlation $r=0.490$ and $r=0.253$, respectively, Fig. 4e). These results show that, indeed, motor dynamics in the value-based risk task were related to inconsistency levels, both in- and out-of-sample.

To check the robustness of these results, we also employed an unsupervised algorithm for reducing the dimensionality of the data. To this end, we conducted a Principal Component Analysis (PCA; see Supplementary Note 6) on the mouse features. Importantly, this method preserves all the mouse features (as opposed to the elastic net), but at the expense of the interpretability of the components. We then used the results from the PCA and examined whether the principal components correlated with inconsistency levels in a subjects fixed-effects regression (Fig. 4b and Supplementary Fig. 5a). The PCA strategy yielded very similar results to the elastic-net approach (Supplementary Note 6 and Supplementary Fig. 5b-c).

To conclude, two analysis approaches, across two independent samples, indicated that motor components during task execution were related to subjects' inconsistent choice behavior on a subject-by-subject level. However, note that the mouse features from the value-based risky-choice task did not capture solely "pure" motor computations. Rather, subjects might have been actively engaging in value computations during the motor trajectory towards the final choice. To demonstrate this, we conducted a regression using the same mouse features as in Fig. 4c but this time on SV (instead of inconsistency level – MMI). Indeed, the Adj-R^2 was relatively high – 17.07% (behavioral study) and 19.82% (neuroimaging study). Accordingly,

relating mouse features from the value-based task to inconsistency levels of the same task is only a partial demonstration of our main goal, which was to quantify inconsistency-related dynamics originating in motor circuits and to disentangle them from those, which originate in value-related crcuits. The next set of analyses addresses exactly this issue.

[Insert Fig. 4 here]

Basic motor traits, unrelated to value modulation, also predict choice inconsistency

Since we aimed to demonstrate that inconsistency was also influenced by the dynamics of motor charateristics originating in noisy computations in neural motor networks unrelated to value-based computations, we wanted to investigate subjects' motor output outside the value-based choice framework. Therefore, following the main risky-choice task, subjects also completed novel non-value tasks (the *Motor task* and the *Numerical task*, Fig. 1a-b, Methods and Supplementary Notes 1-2). Here, too, we recorded mouse trajectories during task execution and extracted the same 34 mouse features that we extracted in the main risky-choice task (Fig. 3, Methods and Supplementary Note 3). We designed the non-value tasks in such a manner that precluded any sort of a valuation process, yet would yield similar motor dynamics to the ones in the main risky-choice task. This design allowed us to relate task execution in the non-value tasks to inconsistency levels in the main risky-choice tasks, which could directly indicate on additional sources for choice inconsistency other than miscalculations of value.

In the *Motor task,* subjects had to reach a predefined circular target marked on a linear graph (similar to the linear budget set) but the graph had no numbers on the axes-grid, whereas in the *Numerical task* subjects had to reach a predefined numerical target coordinate that lied on a linear graph. Importantly, the linear graphs in both non-value tasks were the actual budget lines from the main value task and the location of the predefined targets were identical to the location of the choices each subject made in the main choice task (Fig. 1a middle and right panels).

To measure subjects' precision in the non-value tasks, we calculated the Euclidean distance between the predefined target coordinates and the coordinates of the actual location of the button press (Fig. 2c). We found that subjects were very precise in their button-press loci, which indicates that they had no major difficulties in task execution, and that mouse trajectories from the non-value motor tasks were comparable to trajectories in the main task (see also Supplemnatry Note 5 and Supplementary Fig. 2).

As in the main value-based risky-choice task, we repeated the dimensionality reduction procedure using an elastic net regularization on the mouse features extracted from the non-value tasks and tested whether these features correlated with inconsistency levels estimated in the value-based risk task (Fig. 4b and Methods). Since mouse features in the non-value tasks did not involve any value calculations, they can be regarded as strong out-of-sample predictors of the effect that motor dynamics had on inconsistency levels (Fig. 4b). Importantly, we found that the selected mouse features from the non-value tasks accounted for variation in inconsistency scores in the main risky-choice task. That is, mouse features from the motor task explained 15.5% and 18.6% (behavioral and neuroimaging studies, respectively) of the variance in inconsistency scores, whereas mouse features from the numerical task explained 15.9% of the variance (behavioral study) (Fig. 4d). Note, that even though the adj-R^2s are not as high as when using the mouse features extracted from the main value task, they are still impressively and surprisingly high, given that the regressors are derived from a different task.

Our unique analysis approach, which leverages the mouse features, enabled us to point at the exact motor characteristics that influenced inconsistency scores. Namely, we found that only one feature, the maximal distance from the straight line between the axes'-origin and choice (*MD*), significantly correlated with inconsistency levels across the two studies and all the different tasks. In all analyses, we obtained a positive coefficient for this feature, suggesting that the larger the distance, the higher the inconsistency levels. This suggests that when subjects were wandering around the grid further from the shortest path to their choice, they ended up choosing inconsistently. Furthermore, across the main and motor tasks (in each sample) we also found that the average velocity during the trial (*meanVel*), negatively correlated with inconsistency scores, implying that fast movements led to consistent choices, perhaps indicating that the subject was precisely aiming at a specific location.

Next, to obtain a true cross-tasks prediction, we treated the regression of mouse features from the main value-based task on MMI scores as a training set (the same regressions reported in the previous section). We used the estimated coefficients of the mouse features from this regression (β_i) and applied them to be the coefficients of the mouse features extracted from the non-value tasks, which we considered as our test set. Based on this, we calculated the predicted inconsistency scores for the main risky-choice task using the mouse features extracted from either the motor or numerical tasks ($\hat{Y}$ *or* $\hat{Z}$, for the motor and numerical tasks, respectively, Fig. 5a). We then correlated these predicted inconsistency values with the actual MMI scores and found a significant positive correlation in both the behavioral study (r=0.418 and r=0.393, p<0.0001, motor and numerical tasks, respectively, Fig. 5b) and in the neuroimaging study (r=0.356, p<0.0001, motor task, Fig. 5c). This strengthens our findings that

mouse features from the non-value tasks could predict inconsistency levels in the risky-choice task even when using regression coefficients that were trained on a different dataset.

[Insert Fig. 5 here]

Finally, here, too, we repeated the PCA analysis for all the results reported in Fig. 4d-e and Fig. 5, and found similar findings (Supplementary Note 6 and Supplementary Fig. 5b ,d).

Taken together, using two different tasks that captured motor output but did not involve value modulation, in two different samples with two different analysis approaches including two out-of- sample predictions, we were able to show that choice inconsistency in value-based decision-making is affected by motor dynamics and computations. Our findings suggest that basic motor dynamics contribute 15-20% of the variability in inconsistency scores.

Neuroimaging results

Replication of the main finding from our previous study.

As we hypothesized that neural noise in value brain regions during valuation leading up to a choice is one source for choice inconsistency, we first aimed to replicate the main finding from our previous study[18], which showed that value-modulation and inconsistency levels correlate with the BOLD signal in the same value-related ROIs. We therefore ran the same random-effect general linear model (RFX GLM) used in that study (see Methods), and focused our investigation on pre-hypothesized value-related ROIs. Indeed, we found that MMI correlated with all predefined value ROIs (the ventromedial prefrontal cortex – vmPFC, the ventral striatum – vStr, the dorsal anterior cingulate cortex – dACC and the posterior cingulate cortex – PCC, $p<0.05$, cluster-size corrected, Fig. 6a). We further found a conjunction between regions that correlated with inconsistency and with the subjective value (SV) of the chosen bundle in each trial in three of these regions (vStr, dACC and PCC, $p<0.05$, cluster-size corrected, Fig. 6a). We did not find similar activations in the whole-brain analysis, perhaps since 8 of the subjects in the new sample (19.5%) were fully consistent, which resulted in a weaker correlation of inconsistency levels with the BOLD signal. Another possible explanation is the fact that the current study had lower power[30] compared to the previous study, as each subject completed only 75 trials instead of 108. Therefore, we also ran a less stringent model, which only included reaction time and inconsistency levels as regressors (Methods). Here, we found a positive correlation between MMI and the BOLD signal in the ACC/mPFC in a very similar region to the one we found in the whole-brain analysis in our previous study ($p<0.005$, cluster-size corrected

with 1,000 Monte Carlo iterations, Fig. 6d). These results indicate that we were able to successfully replicate our previous findings in a different sample, confirming that inconsistency emerges during value modulation.

Motor brain regions also correlate with value modulation and inconsistency levels.

Next, we looked at the second hypothesized source of choice inconsistency: neural noise originating from motor planning and execution. We thus tested whether inconsistency levels and valuations correlated with activations in motor brain regions. We ran the same RFX GLM that we conducted in the value-related brain regions, this time on M1 and the supplementary motor area, SMA (see Methods and Supplementary Fig. 6), and found that both these regions correlated with inconsistency levels (SMA – positive correlation, M1 – negative correlation, $p<0.05$, cluster-size correction, Fig. 6b). In line with previous studies, we also identified a strong activation of the SV regressor in these regions, which demonstrates the notion that motor regions receive information regarding valuations from value-related brain areas before execution[31], and/or that this activation is evidence for the representation of action values[32]. Here, too, we saw an overlap between the neural correlates of SV and inconsistency levels ($p<0.05$, cluster-size corrected, Fig. 6b), suggesting that not only did activity in motor brain regions encode valuations of choice, but rather also contributed to inconsistency levels.

Finally, we also examined the activity in V1 as a control region and found a very small cluster in the right hemisphere, which correlated with MMI, and another very small cluster in the left hemisphere, which positively correlated with SV. Nonetheless, given the contralateral correlates of the two regressors, there was no conjunction between them, nor did these findings survive a more stringent threshold (see Methods and Fig. 6c). This suggests that valuations and inconsistency levels were not jointly represented in any main brain region to be tested.

Functional connectivity between motor and value brain regions moderates inconsistency levels.

Next, we wanted to show that choice inconsistency originates from inter-transmission activations between motor and value brain regions. Therefore, we performed a psychophysiological interaction (PPI) functional connectivity analysis (see Methods). We used the value regions (vmPFC, vStr, dACC, and PCC) as seeds and ran a separate PPI regression for each of the two motor regions (M1 and SMA; for a total of 8 models). We found that as MMI increased (more inconsistent), M1 had stronger connectivity with three of the value regions (vStr, dACC and PCC; see Supplementary Table 5). In the SMA, we found a similar result for the dACC seed. These results show that the activity in motor and value brain regions were more synchronized in inconsistent trials than in consistent trials, strengthening the notion that motor-related computations also contributed to inconsistency levels.

[Insert Fig. 6 here]

Neural correlates of mouse features.

We next turned to look at how the mouse features were represented in the brain. Our main goal was to compare the neural correlates of the mouse features during the main value-based risky-choice task to the non-value motor task, and then test whether this representation was related to the degree of inconsistency levels. We first examined mouse features' neural correlates in both value and motor ROIs. We hypothesized that the mouse features would correlate with activity in the motor ROIs in both tasks, as these features reflected the motor dynamics of task execution regardless of the specifics of the task at hand. However, we speculated that mouse features would be evident in value-related ROIs solely during the main value-based risky-choice task, where motor dynamics also reflected the valuation and choice process.

To test this, we ran a RFX GLM on the BOLD signal in the value and motor ROIs using the five mouse features from the behavioral analysis (elastic net, see Fig. 4c bottom panel), which significantly correlated with MMI (meanVel, EndOfTrialVel, MD, AveFixTime and TimeNearPredicted). Fig. 7a presents an overlay of the neural correlates of the mouse features from the elastic net approach in all ROIs in the risky-choice task (Fig. 7a, upper row) and motor task (Fig. 7a, bottom row).

Following our hypothesis, we found that mouse features correlated with activations in the motor ROIs in both the main task and the motor task ($p<0.05$, cluster-size corrected). However, in the value ROIs we found a large discrepancy between the two tasks. While in the risky-choice task we identified that the mouse features strongly correlated with activations in value ROIs (clusters of activations that correlated with mouse features in each ROI: vStr: 4/5 features, dACC: 3/5 features, PCC: 5/5 features, vmPFC: 3/5 features, $p<0.05$, cluster-size corrected), we barley found any representation of the mouse features in value ROIs during the motor task (clusters of activations that correlated with mouse features in each ROI: vStr: 1/5, dACC: 0/5, PCC: 2/5, vmPFC: 1/5, $p<0.05$, cluster-size corrected). In other words, in line with our hypothesis, based on these results, and also demonstrated in the elastic net approach above, neural activations associated with choice dynamics during the motor task, were much weaker in the value ROIs than during the risky-choice task. Furthermore, only during the risky-choice task, we identified similar neural patterns associated with choice dynamics in both motor and value brain regions, which suggests a transmission of motor cues between the two networks, only when task-execution involved a valuation process.

We next aimed to directly associate the neural activations of motor dynamics in the motor brain regions with inconsistency levels, to examine if the relationship we found in behavior between motor dynamics and inconsistency levels also holds at the neural level. To this end, we correlated across subjects the change in the BOLD signal in m1 and SMA ROIs that was attributed to each mouse feature (subject-specific beta coefficients), as estimated in the RFX GLM during the main value task (presented in Fig. 7a, upper row), with the change in the BOLD signal attributed to inconsistency levels (MMI) in the same ROIs (as measured in the RFX GLM presented in Fig. 6b).

We got no significant correlations in m1, perhaps due to the weaker inconsistency signal in that ROI (Fig. 6b). However, we did find significant correlations in the SMA ROI for two mouse features (EndOfTrialVel: $r=0.483$, and MD: $r=-0.424$, $q(FDR)<0.05$) and another feature with a marginally significant correlation (AveFixTime: $r=0.282$, $p=0.07$) (Fig. 7b).

To conclude, the current analysis shows that motor characteristics of task execution had an explicit neural footprint in motor circuits, one which directly affected the neural computation of inconsistent choice behavior. This provides direct evidence for the role of the motor cortex in erroneous choice in value-based decision-making.

[Insert Fig. 7 here]

Ruling out value modulation in the motor task. Finally, to validate that our non-value motor task did not involve any sort of value modulation related to choice, we conducted two separate analyses. First, we conducted an "as-if" analysis, where we treated the location of the button-press in each trial as if it was an actual choice had it been conducted in the value-based risky-choice task. Based on this assumption, we calculated what would have been the inconsistency level and SV had it been a choice in the value-based task (Methods and Fig. 8a). We then looked for the neural correlates of this as-if SV regressor with the BOLD signal in the motor task, using the same RFX GLM modelling that we used in the replication analysis (described in Fig. 6). We found null results for all predefined value ROIs (Fig. 8b, $p<0.05$, cluster-size corrected), indicating that subjects in the motor task did not conduct monetary-based value computations during motor execution, nor did they treat the location of the button-press as choosing a lottery.

In the second analysis, we hypothesized that the motor task carried a different type of decision-making procedure, one that did not include value computations, but rather a different type of computation. We speculated that at each point in time during the trial the subject determined the distance between the mouse curser and the predefined target, indicating

whether she has already reached the predefined target's coordinate (Methods). To this end, in each TR, we calculated the Euclidean distance between the current position of the mouse's curser and the predefined target, and looked for its neural correlates in all value-related ROIs. We found it was negatively correlated with BOLD activations in the vStr, meaning, that the vStr became more active as subjects were closer to the target, probably suggesting a reinforcement-like signal for target-reaching (Fig. 8c, $p<0.05$, cluster-size corrected). This result shows that during the motor task subjects did not calculate subjective value nor tried to maximize utility of chosen lotteries, but instead calculated the spatial location of the mouse relative to the target location.

[Insert Fig. 8 here]

Discussion

In this study, we used behavioral paradigms, neuroimaging, and mouse tracking techniques to show that suboptimal choice is the result of two interacted neural processes. Idiosyncratic choices, leading to violations of fundamental economic axioms, rise during the noisy process of value computation, but at the same time are also influenced by mechanisms of task-execution instantiated by motor output. The current research presents novel modifications to standard mouse-tracking techniques, implemented on a well-established task in risky choice, alongside innovative non-value motor tasks that isolate motor planning and execution from choice dynamics in the same experimental setting.

We find that subjects' inconsistency levels are comparable with previous studies, using the same task[18,19,23], and that subjects do not choose at random. We extracted a total of 34 innovative mouse features from recorded trajectories to characterize temporal and spatial variation in choice dynamics. Controlling for other task parameters, the mouse features accounted for roughly 26% of the variation in inconsistency levels in the behavioral study and 18% in the neuroimaging study. Crucially though, we obtain a close estimate when using mouse features that solely originate from the non-value motor tasks. As these tasks were absent any value-related computations, they solely represent motor planning and execution. We thus argue that 15-20% of the variance in inconsistency levels emerges during task-execution, and originates from motor-related noisy neural processes. We illustrate this finding in two different analytical approaches, with both in- and out-of-sample prediction techniques. Finally, we were able to replicate our previous neuroimaging results[18] and show that inconsistency emerges during the computation of value and is represented in value related brain areas, but at the same

time, is also affected by motor dynamics and activations in motor brain regions. Our behavioral and neural findings tie motor features revealed in task execution to inconsistent choice. This implies that the decision output in our task is not only the result of value computation per se, but is also affected by noise in the motor system.

Several studies have already shown how noisy neuronal computations of value, rather than explore-exploit or diversification strategies, may cause irrationality or imprecision in value-based choice[5,18,33–35]. Similarly, spontaneous neuronal activity also accounts for stochastic choices in sensory and motor decision-making[1,8,36]. In fact, even volatile task-independent neural activations in rest can predict task performance[37], suggesting that unstructured neuronal variation affects behavior. We argue that the neural dynamics that give rise to inconsistent choice are not limited to the value system and go beyond suboptimal valuations. Instead, through interconnected motor-value loops, motor planning and execution have an incremental contribution to irrational choice.

Our work suggests that basic motor traits in task execution account for 15-20% of suboptimality in choice. Previous studies claimed that the contribution of motor noise to variability in choice is much more limited (around 3-5%)[1,5]. One possibility for this discrepancy is that the motor output in our task was longer and more complex (moving the mouse towards a budget line in our task vs. a button-click in a binary-choice task in previous studies). The complex output required greater motor planning and resources that were more susceptive to the accumulation of motor noise, which in turn, led to a greater effect of motor neural circuits on suboptimal choices.

Our findings that velocity (meanVel, EndOfTrialVel), level of directedness (MD), and motor fixations (AveFixTime, TimeNearPredicted) correlated with inconsistency can indicate two different mechanisms (perhaps not mutually exclusive) by which motor dynamics contributed to inconsistency levels: (a) motor noise in execution diverted subjects from their preplanned choice target. The relationship between inconsistency levels and motor features from the motor task strengthens this idea. (b) Subjects continued to deliberate on their final choice after motion onset, and continually updated their course of action until reaching a final decision. The relationship between SV and mouse features, as well as the inter-connected motor-value activations, revealed by the neuroimaging results, can support this notion. Note that both (a) and (b) could result in higher inconsistency levels.

Our neuroimaging findings regarding the neural dynamics associated with motor dynamics in value ROIs during the main risky-choice task indicate that mouse features reflected several aspects of the valuation process, ones that go beyond motor planning and task execution, and thus were also reflected in the value ROIs. This suggests that motor signals

affected the choice process. The fact that both motor and value regions also correlated with inconsistency levels implies that both networks contributed to inconsistency levels. The weaker correlations during the motor task further indicate that the bidirectional transmission between the networks was less necessary in the absence of a value-based choice process.

This can imply that the transmission between decision circuits and motor regions is perhaps not sequential nor is it only feed-forward. Rather, it may reflect a continuous flow of information between circuits[38], which can point at further deliberation after movement onset[39]. In line with these findings, single-unit recordings in primates showed that neurons in the premotor cortex simultaneously encode multiple movement goals before a choice is made, ruling out the possibility of a single distinct sequential transmission from the value network to motor brain regions[40,41].

The only feature that correlated with inconsistency levels across all tasks and samples was MD, the maximal distance from the shortest path to the final choice, which indicated that subjects, who travelled in straight "decisive" pathways towards choice, were less likely to demonstrate high inconsistency levels. This suggests that these routes had lower noise levels and corroborates the groundbreaking work of Harris & Wolpert (1998)[42], who argued that straight trajectories are selected to minimize the variance in end-point positions, as a result of a unimodal velocity profile that minimizes the accumulated signal-dependent noise, which is the cause for deviations from targets[12]. In our study, minimizing the variance towards the end-point also translates into lower inconsistency levels. Since the intensity of inconsistency levels is sometimes referred to as a measure of wasted income[17], these routes can be considered less costly, suggesting that motor planning takes into account subjects' own motor uncertainty which carries monetary costs[43,44].

We study decision mechanisms and task execution using mouse tracking, which captures temporal and spatial choice dynamics with high resolution. Decision dynamics also illuminate deliberation processes between chosen and unchosen options, while indicating the timing and loci of subtask computations[24]. Thus, mouse tracking has been extensively used in recent years to study implicit cognitive mechanisms in several domains, such as social categorization and face recognition[45–47], psycholinguistics[48,49], visual search[50], and memory recognition[51]. Lately, mouse tracking has also been applied to the study of value-based decision-making, including consumer goods and dietary choices[26–28], learning mechanisms[52] and inter-temporal choice[53,54]. This line of studies was followed by rich and exhaustive methodological reports[24,25,55–58], but, to date, has focused only on binary choice tasks. Our study builds upon the standard mouse-tracking methodological framework, and expands it to a task

with a continuum of multiple-choice options. Our metrics can be applied to many other tasks, which use a wide array of choice options.

Finally, going back to the "trembling hand" and the riddle of erroneous choice, economists have long argued that inconsistencies in subjects' responses can be the result of some random component in their preferences ordering[59,60]. More recently, theorists modeled these inconsistencies as resulting from a *deterministic source*[61]. The "constant-error" approach[62] suggested that subjects obey some deterministic theory of choice, but will experience a tremble or a lapse with some probability at the execution of choice. In contrast, the "white noise" approach posed that subjects maximize a utility function with some additive noise term[63,64], implying that stochasticity in choice occurs during the valuation process. This approach was supported by neural evidence, suggesting that the source for these stochastic valuations is the spontaneous fluctuations of neural networks in value-related brain regions[11,18,35]. The current study presented vast empirical evidence that bridges these two schools of thought, and suggests that irrationality can be the result of a combination of two different random neural processes.

Methods

Main risky-choice task. Subjects made choices from linear budget sets in the context of risk[18,19]. On each trial, subjects were presented with a set of 50/50 lotteries between two accounts, X and Y, and were asked to choose their preferred lottery (a bundle of some amount of X and some amount of Y). All possible lotteries in a given trial were represented along a budget line. The price ratios (slopes of the budget lines) and endowments were randomized across trials (see Supplementary Tables 1 and 2 for budget sets' parameters). Importantly, we set the mouse cursor at the axis-origin at the beginning of each trial, and recorded mouse trajectories (see Mouse Tracking below). For further details on the main task, see Supplementary Note 1, the left panel of Fig. 1a and our previous study[18].

Non-value motor tasks. Following the main task, subjects conducted non-value motor tasks, in order to examine motor-related sources of choice inconsistency that did not involve value modulation. We used these tasks to test whether certain characteristics in subjects' motor planning and execution could account for subjects' choice behavior and inconsistencies.

Motor task. Subjects were presented with linear graphs and had to reach a black circular target on the graph. The graphs, nor the axes-grid, presented numbers. When subjects reached the black target, they left-clicked the mouse to submit their position (middle panel of Fig. 1a).

Numerical task. Similarly, the numerical task tested subjects' motion pathways when absent value modulation, though instead of visual circular targets, here, subjects had numerical coordinates as targets. Subjects were presented with linear graphs, and had to reach a predefined $\{x, y\}$ coordinate appearing at the top of the screen, which represented a target spot on the graph (right panel of Fig. 1a). The current $\{x, y\}$ cursor position was presented continuously at the top of the screen. When subjects reached the target coordinate, they left-clicked the mouse/trackball to submit their position.

In both non-value motor tasks, to fully resemble the main task, each graph (both the slope and the endowment) was identical to a graph from the main risky-choice task. The predefined targets for both non-value motor tasks were identical to the actual location on that graph that each subject chose in the main risky-choice task. That is, the loci of the predefined targets were subject-specific. Note that in both tasks there was no value-based decision-making, as the X- and Y-axes did not represent monetary payoffs. Here, too, we set the mouse cursor to the axes-origin at the beginning of each trial, and recorded mouse trajectories. Supplementary Notes 1-2 detail the experimental procedures and provide English versions of the instructions sheet of the non-value motor tasks (behavioral study).

Inconsistency analysis. For a subject-level analysis, we calculated the number of GARP violations[14]. We used AI[17] and MMI[23] to measure the intensity of violations. Similarly to our previous study[18], we implemented a Leave-one-out method on MMI for a trial-by-trial analysis of inconsistency levels, to yield Trial-specific-MMI. See Kurtz-David et al. (2019)[18] and Supplementary Note 4 for further details and formal definitions.

Parametric utility recovery. For each subject, we recovered the subject-specific utility parameters, using Gul's Disappointment Aversion function[65]. To use subjective value (SV) as a parametric regressor in our behavioral and neuroimaging analyses, we calculated the value of the Disappointment Aversion model with CRRA functional form at the chosen bundle (x^i, y^i) in each trial i, using the subject's recovered parameters, β and ρ. See Kurtz-David et al. (2019)[18] and Supplementary Note 4 for further details.

Measuring choice difficulty. For each subject and trial, we calculated the choice simplicity index (CSI), as presented in our previous study[18] (See also Supplementary Note 7). CSI was used as a control variable in the multiple regressions in Approaches A and B.

Mouse tracking preprocessing. We recorded mouse movements using MATLAB built-in functions. Each movement of the mouse triggered writing its location in its $\{x, y\}$ coordinates and a timestamp in a dedicated excel file. Since sampling occurred only when the mouse moved, it resulted in unequal sampling intervals. We used the timestamps and coordinates to interpolate the mouse location in either 100 or 1,000 samples with equal intervals in time (using MATLAB's interp1 function). The total time of a trial differed, so the resulting 100/1,000 samples had different sampling rates per trial, but a constant sampling rate within trial. In addition, for some features we required trajectory samples to represent a fixed curve rather than movement through time. Therefore, we also created a version of each trajectory where samples were evenly spaced on the X and Y axes, neglecting the time domain. In this case, the number of samples per trajectory was determined as half the total distance travelled in the trial (in coordinates units), to create a coherent and smooth representation of the trajectory curve. All features reported in this study were extracted on either the evenly spaced trajectory curve, the 100 mouse trajectory samples with equal time-intervals, or the 1,000-samples trajectory, which provided higher temporal resolution and enabled more precise calculations in certain features. Trajectories with two samples or lower could not be analysed and were discarded. This was caused by faulty sampling or a hastened miss-click by the subject, and occurred only in 1 trial in the risky-choice task, 13 trials in the numerical cognition task and 29 trials in the motor task (behavioural study). In the neuroimaging study, this did not occur, so no trials were excluded due to a low number of samples.

Extracting mouse features. We characterized each mouse trajectory using multiple features, in order to extract as much information as possible on the decision process and task execution, from various aspects and approaches. Since we did not know ex-ante which features would relate to either value modulation or motor processes, we aimed to extract a large variety of features. Many features were based on or inspired by Jonathan B. Freeman's extensive work on mouse trajectories, such as maximum deviation (MD), complexity (axis-flips), velocity, acceleration, and area under the curve (AUC), adapted to our experimental design[24,25,55,56,66]. We also calculated the trajectory angle at each time point, with respect to a straight line from the axes origin towards the chosen bundle, adapted from a work by Sullivan and colleagues[26]. Additionally, we used sample entropy[67] to discern the complexity of trajectories (see Feldman & Crutchfield (1998)[68] for a discussion of complexity measures). For the purpose of extracting trajectory curvatures at each time point we employed an open-source MATLAB code for curvature calculation, on the evenly spaced trajectory curve[69]. Other features, such as features related to mouse fixations and layover at the axis' origin, or features concerned with the time spent in different areas relative to the budget set (i.e., time out of the grid bounds, time above budget line, time near the predicted bundle and time on budget line), were our own design.

We extracted a total of 34 mouse features from recorded trajectories. A comprehensive list of all the features we used appears in Supplementary Table 3, while a more detailed account on the extraction of each feature appears in Supplementary Note 3.

Dimensionality reduction. Due to the high number of mouse features relative to the number of trials (both studies), and due to inter-features' correlations, we had to induce dimensionality reduction. To this end, we took two different strategies: *Approach A:* feature selection via elastic net, a linear combination of the Ridge and Lasso regularized regression methods (performed in STATA); *Approach B:* a feature projection strategy via PCA. The main advantage of the elastic net approach is that it allows for a straightforward interpretation of the results on the expense of losing some information concealed in the features that did not survive the regularization. On the contrary, the PCA approach maintains all mouse-features' data, but loses some of the interpretability. We implemented these two strategies in mouse features from the main risky-choice task (z-scored) in each of our two studies.

The elastic net analysis was run against inconsistency levels (MMI) and included subjects fixed-effects with 10 folds cross-validation. A total of 28 features survived the regularization in the behavioral study ($\alpha = 1.0, (Lasso), \lambda = 2.266, MPSE = 0.0029\alpha$) and a respective group of 10 features survived the regularization in the neuroimaging study ($\alpha = 0.8, \lambda = 149.00, MPSE = 0.965$), out of which 15 and 5 features (behavioral and neuroimaging studies, respectively) correlated with MMI. The list of surviving features appears in

Supplementary Table 4. See Supplementary Note 6 for the PCA dimensionality reduction strategy.

Relating choice dynamics to inconsistency levels. Following dimensionality reduction, we tested whether choice dynamics could predict inconsistency levels, using a subjects fixed-effects regression on motor components:

$$(1)\ MMI_i^s = \beta_0 + \beta_k SelectedFeature_k + SID + \theta + \varepsilon$$

where $s \in \{1, \dots, 89\}$ in the behavioral study and $s \in \{1, \dots, 42\}$ in the neuroimaging study is an index indicating subjects' identity, i is an index indicating the trial number, $k \in \{1, \dots, 15\}$ in the behavioral study and $k \in \{1, \dots, 5\}$ in the neuroimaging study is an index indicating the mouse features that survived the elastic net regularization. SID is a subjects-fixed effect and θ is a vector of control variables including SV, budget set parameters, RT and the CSI index. We ran this model, with and without θ, on the data collected in each study using the mouse features from the risky-choice task. See Supplementary Note 6 for the models used in the PCA strategy.

Leave-one-subject-out procedure. To obtain an out-of-sample prediction between mouse-tracking data and inconsistency levels, we estimated regression coefficients for $n - 1$ subjects (same model as in the previous paragraph), and predicted inconsistency levels for the nth subject based on the estimated coefficients. We then correlated these predicted values with the actual MMI scores across subjects.

Relating motor output from the non-value motor tasks to choice inconsistency. To evaluate whether motion components unrelated to value modulation also correlated with inconsistency scores, we repeated the dimensionality reduction process on mouse features from the non-value motor tasks (in each of the two studies). We then used the independent motor components from the non-value tasks to predict MMI scores in the main risky-choice task in a subjects fixed-effects regression. Note that for the purpose of this analysis, in the behavioral study we could only use the subset of 51 trials that were common across the three tasks, whereas in the neuroimaging study all 75 trials were common across tasks and thus all 75 trials were used in this analysis (Fig. 4b).

In the elastic net strategy, we ran the following model:

$$(2)\ MMI_i^s = \beta_0 + \beta_k SelectedFeature_{k,task} + SID + \theta + \varepsilon$$

where $task \in \{motor, numerical\}$ indicates whether the mouse feature was obtained in the numerical or motor tasks. All other notations are identical to equation (1). We ran this model, with and without θ, on the data collected in each study (separately) using mouse features from each of the non-value motor tasks (in separate models) as predictors of inconsistency levels.

We evaluate goodness of fit by examining the adj-R^2 of each model (see Supplementary Note 6 for the models used in the PCA strategy).

fMRI data preprocessing. BrainVoyager QX (Brain Innovation) was used for image analysis, with additional analyses performed in MATLAB (MathWorks). Functional images were sinc-interpolated in time to adjust for staggered slice acquisition, corrected for any head movement by realigning all volumes to the first volume of the scanning session using six-parameter rigid body transformations, and de-trended and high-pass filtered to remove low-frequency drift in the fMRI signal. Spatial smoothing with a 6-mm FWHM Gaussian kernel was applied to the fMRI images. Images were then co-registered with each subject's high-resolution anatomical scan and normalized using the Montreal Neurological Institute (MNI) template. All spatial transformations of the functional data used trilinear interpolation.

Functional ROIs. We focused our analysis on predefined hypothesis-driven regions of interest (ROIs). To maintain continuity with our previous work, all value-related brain regions (vmPFC, dACC, vStr and PCC) were defined in the same way as in Kurtz-David et al.[18]. We used V1 as a control region to rule out the possibility that SV and MMI correlated with a vast number of brain regions. We drew 12-mm spheres around the peak voxels (one for each hemisphere) that were reported in the atlas by Fan et al.[70]

To define the motor brain regions, left-M1 and SMA, we used a degenerated version of the motor task that appeared in our previous study[18] as an independent functional localizer. We estimated a general linear model (GLM) with one predictor that modeled RT using a boxcar epoch function convolved with the canonical hemodynamic response function (HRF), whose duration was equal to the RT of the trial. Six motion-correction parameters and the constant were included as nuance regressors of no interest to account for head motion-related artifacts. We used a stringent Bonferroni correction as a statistical threshold, and defined any significant voxel with a positive correlation as either belonging to M1 or the SMA regions. Finally, to avoid overlapping between ROIs, we excluded from the SMA ROI any voxels that were common with the neighboring dACC ROI. See Supplementary Fig. 6 to see the resulting M1 and SMA functional ROIs.

Neural correlates of choice inconsistency and replication of the main finding in Kurtz-David et al. To identify the neural correlates of choice inconsistency in the main task, we ran exactly the same GLM regression that appeared in our previous study (see Kurtz-David et al. for further details)[18]. Model regression:

$$(3)\ BOLD = \beta_0 + \beta_1 RT + \beta_2 MMI_{trial_specific} + \beta_3 SV + \beta_4 slope + \beta_5 endowment + \varepsilon$$

We tested the model on all our predefined value-related ROIs. Furthermore, we used the same model to examine neural correlates of choice inconsistency and value modulation in M1 and SMA.

Since a large portion of our sample (8 out of 42 subjects, 19%) was completely consistent with GARP, we wanted to increase statistical power for a whole-brain analysis. Hence, we also ran a more refined model, which only included trial-specific-MMI and a boxcar epoch function to model RT, both were entered for the trial duration and convolved with the canonical HRF. Six motion-correction parameters and the constant were included as regressors of no interest to account for motion-related artifacts.

Neural correlates of mouse features. To evaluate the neural correlates of motor output during task execution, we ran an RFX GLM with motor features that survived the elastic net regularization as our predictors of interest (Fig. 4c, bottom). Additional predictors included budget sets parameters (slopes and endowments) and a boxcar epoch function to capture RT. All predictors were normalized, convolved with the HRF and entered for the trial duration. Six nuance head movements regressors and a constant were included as well. We ran the model on each of the value and motor-related ROIs, and looked for differences in the neural representation of motor output between the value-based task compared with the motor task.

PPI. We performed a PPI analysis[71] to examine the changes of task-related connectivity between value and motor brain regions as a function of inconsistency levels. The value related ROIs were selected as seeds (vmPFC, vStr, dACC and PCC) and two separate PPI analyses were done for each seed, one for each motor ROI (M1 and SMA, for a total of 8 models). The PPI regressors were thus generated by multiplying the demeaned BOLD time series of M1 or SMA with the trial-specific MMI (convolved with the canonical HRF). The other regressors that were included in the model are: motor regions' demeaned BOLD time series, MMI, budget sets parameters (slopes and endowments) and a boxcar epoch function to capture RT. All predictors except the BOLD signal were convolved with the HRF and entered for the trial duration. We used the Bonferroni correction for multiple comparisons (8 models), and report significant results of the PPI regressors for a threshold of 0.00625.

Ruling out value modulation in the motor task. To show that our task manipulation worked, and that the additional non-value motor task indeed did not involve value modulation and solely examined motor output, we conducted two separate analyses.

First, we conducted an "as if" analysis and treated the motor task in the neuroimaging study *as if* it actually was a value-based choice task. Given this thought experiment, we treated the coordinates of each mouse button-press at the end of the trial like a lottery chosen in the

main risky-choice task. We then elicited subject-specific utility parameters and calculated the "trial-specific-SV" and "trial-specific-MMI" to be used as parametric regressors in a GLM with a design matrix identical to the GLM used to look for the neural correlates of choice inconsistency in the main task (see above). We ran this model against the BOLD signal in all predefined value-related ROIs. Our main hypothesis in this analysis was to find null positive correlates between the "SV" predictor and the BOLD signal in value-related brain regions, suggesting that the motor task did not result in value modulation processes in the brain (Fig. 6b).

Our second approach was to test whether the motor task induced a different type of decision-making mechanism, one that did not involve utility maximization, nor could it yield choice inconsistencies. We hypothesized that during task execution, subjects had to constantly determine whether they have reached the target coordinate. We therefore used the equal-time sampled trajectories ("InterTime", see Supplementary Note 3) upon which we calculated the exact mouse-location in each TR using a linear interpolation. We then calculated for each such location the Euclidean distance between current location and target. The Euclidean distance between current location and target at each TR was used as a parametric regressor in an RFX GLM, normalized and convolved with the HRF. Additional predictors included the slope and Y-axis intersection of the linear graph, as well as an epoch function to capture RT (all normalized and convolved with the HRF). This model was tested against all the predefined value/decision-making ROIs to look for brain regions that tracked distance from target as a reinforcement-like signal.

Data & code availability

The computer code used for the computation of MMI and the other inconsistency indices is available as an open source code at https://github.com/persitzd/RP-Toolkit. The code package used to generate all mouse features, as well as the datasets generated and analyzed for the current study, the statistical maps and the rest of the computer code used to analyze further behavioral results and the imaging data will be uploaded upon publication to OSF.

References

1. Drugowitsch, J. *et al.* Computational Precision of Mental Inference as Critical Source of Human Choice Suboptimality. *Neuron* **92**, 1398–1411 (2016).

2. Renart, A. & Machens, C. K. Variability in neural activity and behavior. *Curr. Opin. Neurobiol.* **25**, 211–220 (2014).

3. Selten, R. Reexamination of the Perfectness Concept for Equilibrium Points in Extensive Games. *Int. J. Game Theory* **4**, 25–55 (1975).

4. Daw, N. D., O'Doherty, J. P., Dayan, P., Seymour, B. & Dolan, R. J. Cortical substrates for exploratory decisions in humans. *Nature* **441**, 876–879 (2006).

5. Findling, C., Skvortsova, V., Dromnelle, R., Palminteri, S. & Wyart, V. Computational noise in reward-quided learning drives behavioral variability in volatile environments. *Nat. Neurosci.* 1–9 (2019) doi:10.1038/s41593-019-0518-9.

6. Behrens, T. E. J., Woolrich, M. W., Walton, M. E. & Rushworth, M. F. S. Learning the value of information in an uncertain world. *Nat. Neurosci.* **10**, 1214–1221 (2007).

7. Faisal, a A., Selen, L. P. J. & Wolpert, D. M. Noise in the nervous system. *Nat. Rev. Neurosci.* **9**, 292–303 (2008).

8. Lebovich, L., Darshan, R., Lavi, Y., Hansel, D. & Loewenstein, Y. Intrinsic stochasticity in neuronal dynamics. *Nat. Hum. Behav.* **3**, 1190–1202 (2019).

9. Glimcher, P. W. Indeterminacy in Brain and Behavior. *Annu. Rev. Psychol.* **56**, 25–56 (2005).

10. Gold, J. I. & Shadlen, M. N. The Neural Basis of Decision Making. *Trends Neurosci.* (2007) doi:10.1146/annurev.neuro.29.051605.113038.

11. Webb, R. The (Neural) Dynamics of Stochastic Choice. *Manage. Sci.* (2018).

12. Christopher M. Harris & M.Wolpert, D. Signal-dependent noise determines motor planning. *Nature* **394**, 780–784 (1998).

13. Fox, M. D., Snyder, A. Z., Vincent, J. L. & Raichle, M. E. Intrinsic Fluctuations within Cortical Systems Account for Intertrial Variability in Human Behavior. *Neuron* **56**, 171–184 (2007).

14. Afriat, S. N. The Construction of Utility Functions from Expenditure Data. *Int. Econ. Rev. (Philadelphia).* **8**, 67–77 (1967).

15. Houthakker, H. S. Revealed Preference and the Utility Function. *Economica* **17**, 159–174 (1950).

16. Varian, H. R. The Nonparametric Approach to Demand Analysis. *Econometrica* **50**, 945–973 (1982).

17. Afriat, S. N. On a System of Inequalities in Demand Analysis: An Extension of the Classical Method. *Int. Econ. Rev. (Philadelphia).* **14**, 460–472 (1973).

18. Kurtz-David, V., Persitz, D., Webb, R. & Levy, D. J. The neural computation of inconsistent choice behavior. *Nat. Commun.* **10**, 1–14 (2019).

19. Choi, S., Fisman, R., Gale, D. & Kariv, S. Consistency and heterogeneity of individual behavior under uncertainty. *Am. Econ. Rev.* **97**, 1921–1938 (2007).

20. Fisman, R., Kariv, S. & Markovits, D. Individual preferences for giving. *Am. Econ. Rev.*

97, 1858–1876 (2007).

21. Kahneman, D. & Tversky, A. *Choiches, values & frames*. (Cambridge University Press, 2000).

22. Choi, S., Fisman, R., Gale, D. & Kariv, S. Revealing Preferences Graphically : An Old Method Gets a New Tool Kit. *Am. Econ. Rev.* **97**, 153–158 (2007).

23. Halevy, Y., Persitz, D. & Zrill, L. Parametric Recoverability of Preferences. *J. Polit. Econ.* **126**, (2019).

24. Freeman, J. B. Doing Psychological Science by Hand. *Curr. Deirectories Psychol. Sci.* **27**, 315–323 (2018).

25. Freeman, J. B., Dale, R. & Farmer, T. A. Hand in motion reveals mind in motion. *Front. Psychol.* **2**, 1–6 (2011).

26. Sullivan, N., Hutcherson, C., Harris, A. & Rangel, A. Dietary Self-Control Is Related to the Speed With Which Attributes of Healthfulness and Tastiness Are Processed. *Psychol. Sci.* **26**, 122–134 (2015).

27. Stillman, P. E., Medvedev, D. & Ferguson, M. J. Resisting Temptation : Tracking How Self-Control Conflicts Are Successfully Resolved in Real Time. *Psychol. Sci.* **28**, 1240–1258 (2017).

28. Lim, S., Penrod, M. T., Ha, O., Bruce, J. M. & Bruce, A. S. Calorie Labeling Promotes Dietary Self-Control by Shifting the Temporal Dynamics of Health- and Taste-Attribute Integration in Overweight Individuals. *Psychol. Sci.* **29**, 447–462 (2018).

29. Halevy, Y., Persitz, D. & Zrill, L. Parametric Recoverability of Preferences. *J. Polit. Econ.* **126**, 1558–1593 (2018).

30. Bronars, S. G. The Power of Nonparametric Tests of Preference Maximization. *Econometrica* **55**, 693–698 (1987).

31. Hare, T. A., Schultz, W., Camerer, C. F., Doherty, J. P. O. & Rangel, A. Transformation of stimulus value signals into motor commands during simple choice. *Proc. Natl. Acad. Sci.* **108**, 18120–18125 (2011).

32. Wunderlich, K., Rangel, A. & O'Doherty, J. P. Neural computations underlying action-based decision making in the human brain. *Proc. Natl. Acad. Sci. U. S. A.* **106**, 17199–17204 (2009).

33. Padoa-Schioppa, C. Neuronal origins of choice variability in economic decisions. *Neuron* **80**, 1322–1336 (2013).

34. Polanía, R., Moisa, M., Opitz, A., Grueschow, M. & Ruff, C. C. The precision of value-based choices depends causally on fronto-parietal phase coupling. *Nat. Commun.* **6**, (2015).

35. Webb, R., Glimcher, P. W., Levy, I., Stephanie, C. & Rutledge, R. B. Neural Random Utility : Relating Cardinal Neural Observables to Stochastic Choice Behaviour. *J. Neurosci. Psychol. Econ.* Forthcoming (2018).

36. Fox, M. D. & Raichle, M. E. Spontaneous fluctuations in brain activity observed with functional magnetic resonance imaging. *Nat. Rev. Neurosci.* **8**, 700–711 (2007).

37. Finn, E. S. *et al.* Functional connectome fingerprinting: Identifying individuals using patterns of brain connectivity. *Nat. Neurosci.* **18**, 1664–1671 (2015).

38. Selen, L. P. J., Shadlen, M. N. & Wolpert, D. M. Deliberation in the Motor System : Reflex

Gains Track Evolving Evidence Leading to a Decision. *J. Neurosci.* **32**, 2276–2286 (2012).

39. Burk, D., Ingram, J. N., Franklin, D. W., Shadlen, M. N. & Wolpert, D. M. Motor Effort Alters Changes of Mind in Sensorimotor Decision Making. *PLoS One* **9**, 1–10 (2014).

40. Cisek, P., Kalaska, J. F. & Physiologie, D. De. Neural Correlates of Reaching Decisions in Dorsal Premotor Cortex : Specification of Multiple Direction Choices and Final Selection of Action. *Neuron* **45**, 801–814 (2005).

41. Klaes, C., Westendorff, S., Chakrabarti, S. & Gail, A. Article Choosing Goals , Not Rules : Deciding among Rule-Based Action Plans. *Neuron* **70**, 536–548 (2011).

42. Christopher M. Harris & M.Wolpert, D. Signal-dependent noise determinesmotorplanning Christopher. *Nature* **394**, 780–784 (1998).

43. Zhang, H., Maddula, S. V & Maloney, L. T. Planning routes across economic terrains : maximizing utility , following heuristics. *Front. Psychol.* **1**, 1–10 (2010).

44. Trommershäuser, J., Maloney, L. T. & Landy, M. S. Statistical decision theory and trade-offs in the control of motor response. *Spat. Vis.* **16**, 255–275 (2003).

45. Stolier, R. M. & Freeman, J. B. Neural pattern similarity reveals the inherent intersection of social categories. *Nat. Neurosci.* **19**, 795–797 (2016).

46. Stolier, R. M. & Freeman, J. B. A neural mechanism of social categorization. *J. Neurosci.* **37**, 5711–5721 (2017).

47. Freeman, J. B. & Ambady, N. Hand movements reveal the time-course of shape and pigmentation processing in face categorization. *Psychon. Bull. Rev.* **18**, 705–712 (2011).

48. Spivey, M. J., Grosjean, M. & Knoblich, G. Continuous attraction toward phonological competitors. *Proc. Natl. Acad. Sci. U. S. A.* **102**, 10393–10398 (2005).

49. Hindy, N. C., Hamilton, R., Houghtling, A. S., Coslett, H. B. & Thompson-Schill, S. L. Computer-mouse tracking reveals TMS disruptions of prefrontal function during semantic retrieval. *J. Neurophysiol.* **102**, 3405–3413 (2009).

50. Song, J. H. & Nakayama, K. Target selection in visual search as revealed by movement trajectories. *Vision Res.* **48**, 853–861 (2008).

51. Dale, R., Kehoe, C. & Spivey, M. J. Graded motor responses in the time course of categorizing atypical exemplars. *Mem. Cogn.* **35**, 15–28 (2007).

52. Konovalov, A. & Krajbich, I. Mouse tracking reveals structure knowledge in the absence of model-based choice. *Nat. Commun.* **11**, 1–9 (2020).

53. Scherbaum, S., Dshemuchadse, M., Leiberg, S. & Goschke, T. Harder than expected: Increased conflict in clearly disadvantageous delayed choices in a computer game. *PLoS One* **8**, (2013).

54. Dshemuchadse, M., Scherbaum, S. & Goschke, T. How decisions emerge: Action dynamics in intertemporal decision making. *J. Exp. Psychol. Gen.* **142**, 93–100 (2013).

55. Hehman, E., Stolier, R. M. & Freeman, J. B. Advanced mouse-tracking analytic techniques for enhancing psychological science. *Gr. Process. Intergr. Relations* **18**, 384–401 (2015).

56. Freeman, J. B. & Ambady, N. MouseTracker : Software for studying real-time mental processing using a computer mouse-tracking method. *Behav. Res. Methods* **42**, 226–241 (2010).

57. Calcagnì, A., Lombardi, L. & Sulpizio, S. Analyzing spatial data from mouse tracker methodology: An entropic approach. *Behav. Res. Methods* **49**, 2012–2030 (2017).

58. Zgonnikov, A., Aleni, A., Piiroinen, P. T., O'Hora, D. & di Bernardo, M. Decision landscapes: Visualizing mouse-tracking data. *R. Soc. Open Sci.* **4**, (2017).

59. Becker, G. M., DeGroot, M. H. & Marschk, J. Stochastic Models of Choice Behavior. *Behav. Sci.* **8**, 41–55 (1963).

60. Manski, C. F. No Title. *Theory Decis.* **8**, 229–230 (1977).

61. Hey, J. D. Why we should not be silent about noise. *Exp. Econ.* **345**, 325–345 (2005).

62. Harless, B. Y. D. W. & Camerer, C. F. The Predictive Utility of Generalized Expected Utility Theories. *Econometrica* **62**, 1251–1289 (1994).

63. McFadden, D. Economic Choices. *Am. Econ. Rev.* **91**, 351–378 (2001).

64. Hey, J. D. . & Orme, C. Investigating Generalizations of Expected Utility Theory Using Experimental Data. *Econometrica* **62**, 1291–1326 (1994).

65. Gul, F. A Theory of Disappointment Aversion. *Econometrica* **59**, 667–686 (1991).

66. Freeman, J. B. & Dale, R. Assessing bimodality to detect the presence of a dual cognitive process. *Behav. Res. Methods* **45**, 83–97 (2013).

67. Richman, S. J. & Moorman, J. R. Physiological time-series analysis using approximate entropy and sample entropy. *Am. J. Physiol.* **278**, H2039–H2049 (2000).

68. Feldman, D. P. & Crutchfield, J. P. Measures of statistical complexity: Why? *Phys. Lett. Sect. A Gen. At. Solid State Phys.* **238**, 244–252 (1998).

69. Mjaavatten, A. Curvature of a 2D or 3D curve. (https://www.mathworks.com/matlabcentral/fileexchange/69452-curvature-of-a-2d-or-3d-curve), MATLAB Central File Exchange. Retrieved July 1, 2020. (2020).

70. Fan, L. *et al.* The Human Brainnetome Atlas: A New Brain Atlas Based on Connectional Architecture. *Cereb. Cortex* **26**, 3508–3526 (2016).

71. Friston, K. J. *et al.* Psychophysiological and Modulatory Interactions in Neuroimaging. *Neuroimage* **6**, 218–229 (1997).

Acknowledgements

We thank P. Glimcher and D. Persitz for thoughtful comments, D. Hasson for his help in running the behavioral study and O. Nofekh for help with the inconsistency indices code package. This work was funded with a grant from the Israel Science Foundation (#954/17 for D.J.L) and the financial support of the Henry Crown Institute of Business Research in Israel.

Author contributions

V.K.D. and D.J.L conceived the study. D.J.L, A.H. and V.K designed the study. V.K. collected and analyzed the data from both studies. A.H. extracted the mouse features. A.M. performed neuroimaging analyses .N.P. helped with fMRI data preprocessing. V.K.D., A.H, A.M. & D.J.L wrote the manuscript.

Figures

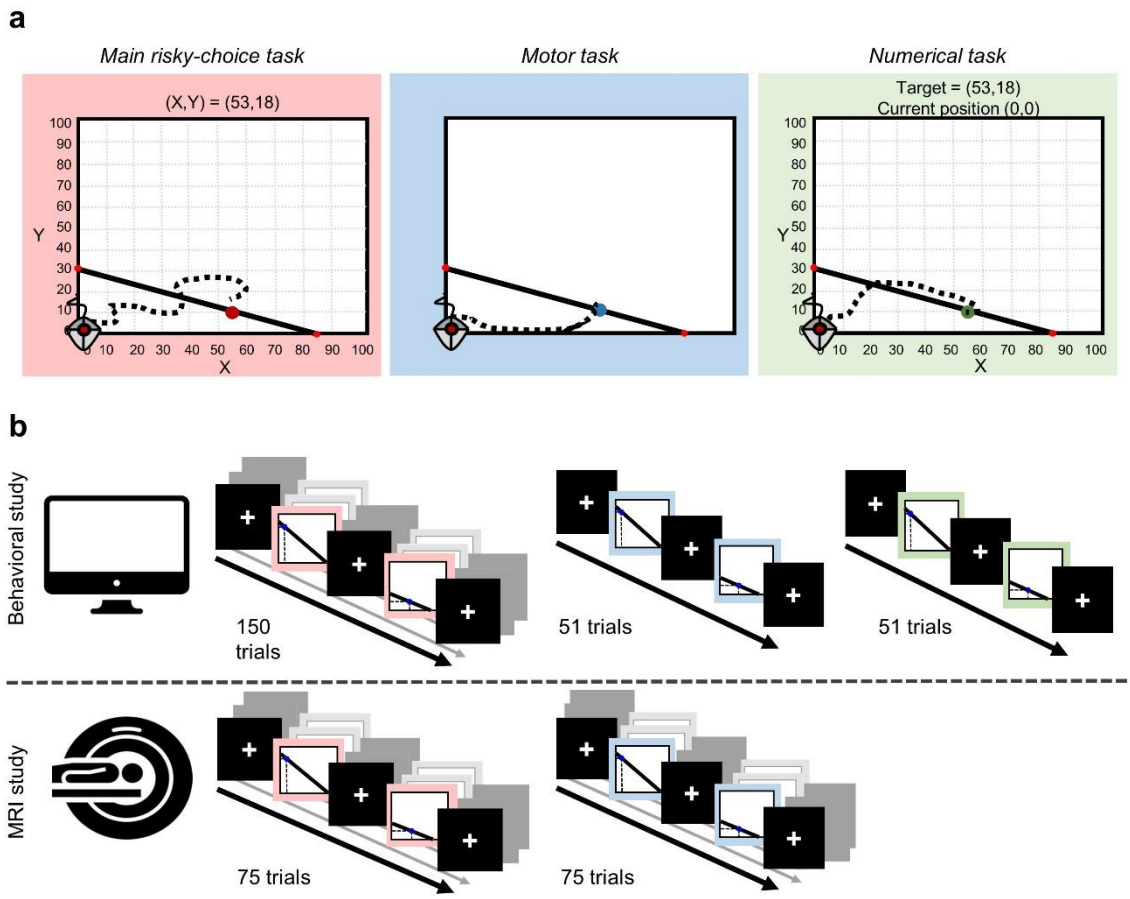

Fig. 1 | Experimental design. (a) In all tasks, at the beginning of each trial we set the mouse cursor at the axes-origin, and recorded mouse trajectories during the trial. In the behavioral study subjects used a mouse while in the fMRI study they used a trackball to submit their choices. *Main task (left).* Subjects were presented with a budget line with 50/50 lotteries between two accounts, labeled X and Y. Each point on the budget line represented a different lottery between the X and Y accounts. Subjects had to choose their preferred lottery (a bundle of the X and Y accounts) out of all possible lotteries along the line. For example, the bundle (53,18, red dot) corresponds to a lottery with a 50% chance to win 53 tokens (account X), and a 50% chance to win 18 tokens (account Y). Each trial presented a different budget line with a different slope (price ratio between X and Y) and endowment, which were randomized across trials. *Middle and right panels.* Non-value motor tasks, aimed to study motor output, absent value-based decision-making. The lines and predefined targets were the budget lines and actual choices from the main task, respectively. *Motor task* (middle, used in both the behavioral and neuroimaging studies). Subjects had to move the cursor to the predefined blue target. Note, that no numerical information was presented, therefore not available for subjects to guide their choices. *Numerical task (right,* used solely in the behavioral study). Subjects had to reach the predefined $\{X, Y\}$ target coordinates. The title displayed subjects' current position. See also Methods and Supplementary Notes 1-2. (b) Experimental procedures. *Upper panel* - in the behavioral study (n=89), subjects completed 150 trials of the main task divided to 3 blocks of 50 trials, followed by one block of 51 trials in each of the non-value tasks (counter-balanced across subjects). *Bottom panel* – in the neuroimaging study (n=42), subjects completed 75 trials in the main and in the motor tasks, each divided to 3 blocks of 25 trials.

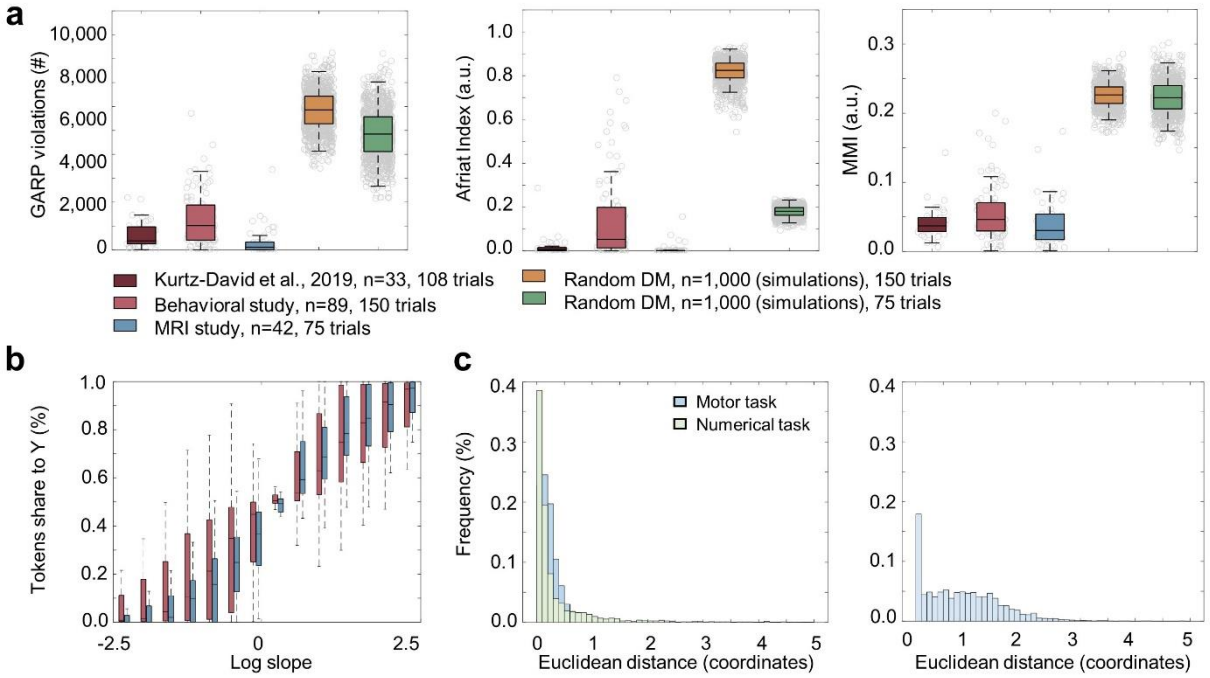

Fig. 2 | Inconsistency levels and imprecision in the non-value motor tasks. (a) Distributions of inconsistency indices among subjects in the two studies, and compared to subjects in our previous study[18] and 1,000 simulated random decision-makers[30]. In the behavioral study (pink bars), only 3 subjects (out of 89, 3.4%) were fully consistent with GARP. Subjects made on average 1,509.1 GARP violations (min=0, max=8,258, std = 2,036.0). Subjects had an average AI score of 0.128 (min=0, max=0.572, std=0.113) and an MMI score of 0.058 (min=0.001, max=0.200, std=0.042). In the neuroimaging study (blue bars), 8 subjects (out of 42, 19.0%) were fully consistent with GARP. Subjects made on average 91.0 GARP violations (min=0, max=1,568, std = 289.5) with an average AI score of 0.037 (min=0, max=0.336, std=0.006) and an MMI score of 0.040 (min=0.001, max=0.174, std=0.036). (b) Subjects obeyed the law of demand. The share of total endowment (expenditure) subjects allocated to the Y account as a function of the price ratio ($^{p_y}/_{p_x}$), the slope of the budget set, increased as the Y account became cheaper. Price ratios are grouped into 15 bins. (c) Distributions of Euclidean dist. (in coordinate units) between target coordinates and the coordinates of mouse-button presses in the non-value tasks. Euclidean dist. could range between 0 and 141.42 (representing the longest diagonal within the axes' grid). *Left* - Behavioral study. Motor task – mean: 0.597, std: 3.403, min: 0, max: 75.479; Numerical task – mean: 0.784, std: 4.670, min: 0, max: 116.885; *Right* - Neuroimaging study: motor task - mean: 0.849, std: 0.795, min: 0, max: 14.677). Distributions of Euclidean distances are highly asymmetrical and skewed at 0, suggesting very high accuracy rates and similar button-press coordinates across tasks. Note that the Euclidean distances in the neuroimaging study (right panel) are higher than in the behavioral study (left panel, $p<0.0001$, Wilcoxon rank-sum test), probably due to some difficulty to maneuver the trackball inside the MRI scanner. Dashed error bars indicate one std.

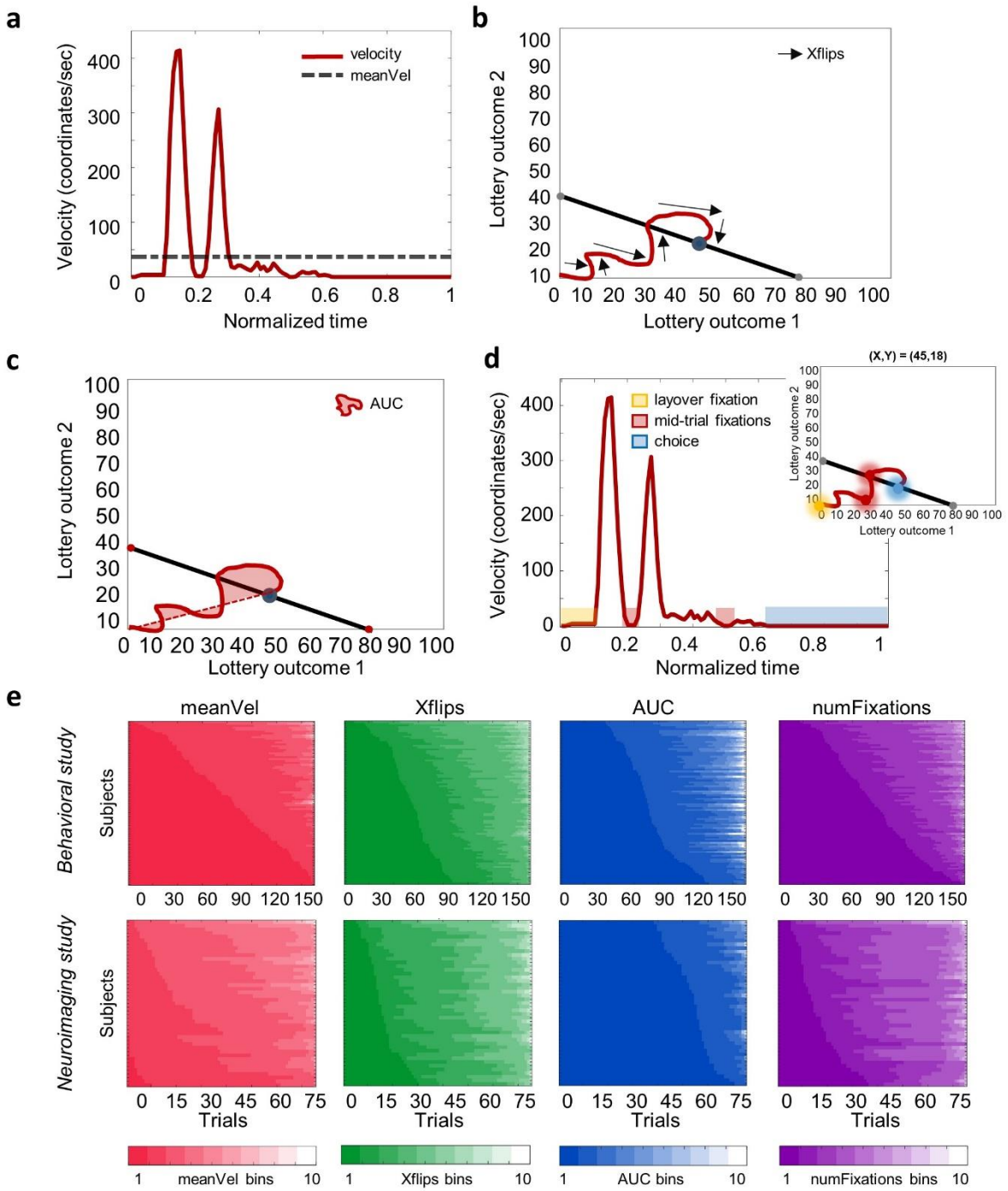

Fig. 3 | Mouse features. (a-d) Representative features (See Methods, Supplementary Table 3 and Supplementary Note 3). (a) *MeanVel* – for each trial we measured the average velocity (dashed line) in coordinates/second (same trial as in Supplementary Fig. 2a, left panel). (b) *Xflips* – in each trial, we measured the number of changes in movement direction (flips) along the x-axis. (c) *AUC* – in each trial we calculated the area confined between the actual mouse trajectory and the "choice line" – the shortest line connecting the axes origin and choice location. (d) *NumFixations*– in each trial, we divided the graph to a 20x20 grid, such that each bin had a width of 5 tokens. Any bin in which the subject spent more than 0.2 seconds was considered a "mouse fixation", meaning segments in which the subject ceased motion, excluding the actual choice. In the NumFixations feature, we count the number of such segments. Figure inset – spatial illustration of mouse fixations. (e) Distributions of trials based on features' values (same features as in a-d). We grouped features into 10 equally-spaced bins. Subjects are sorted by ascending order according to their share of trials classified to bin 1 (lowest values). Within subject (each row), trials are sorted by bins in an ascending order. (*Up* - behavioral study, *Bottom* – neuroimaging study).

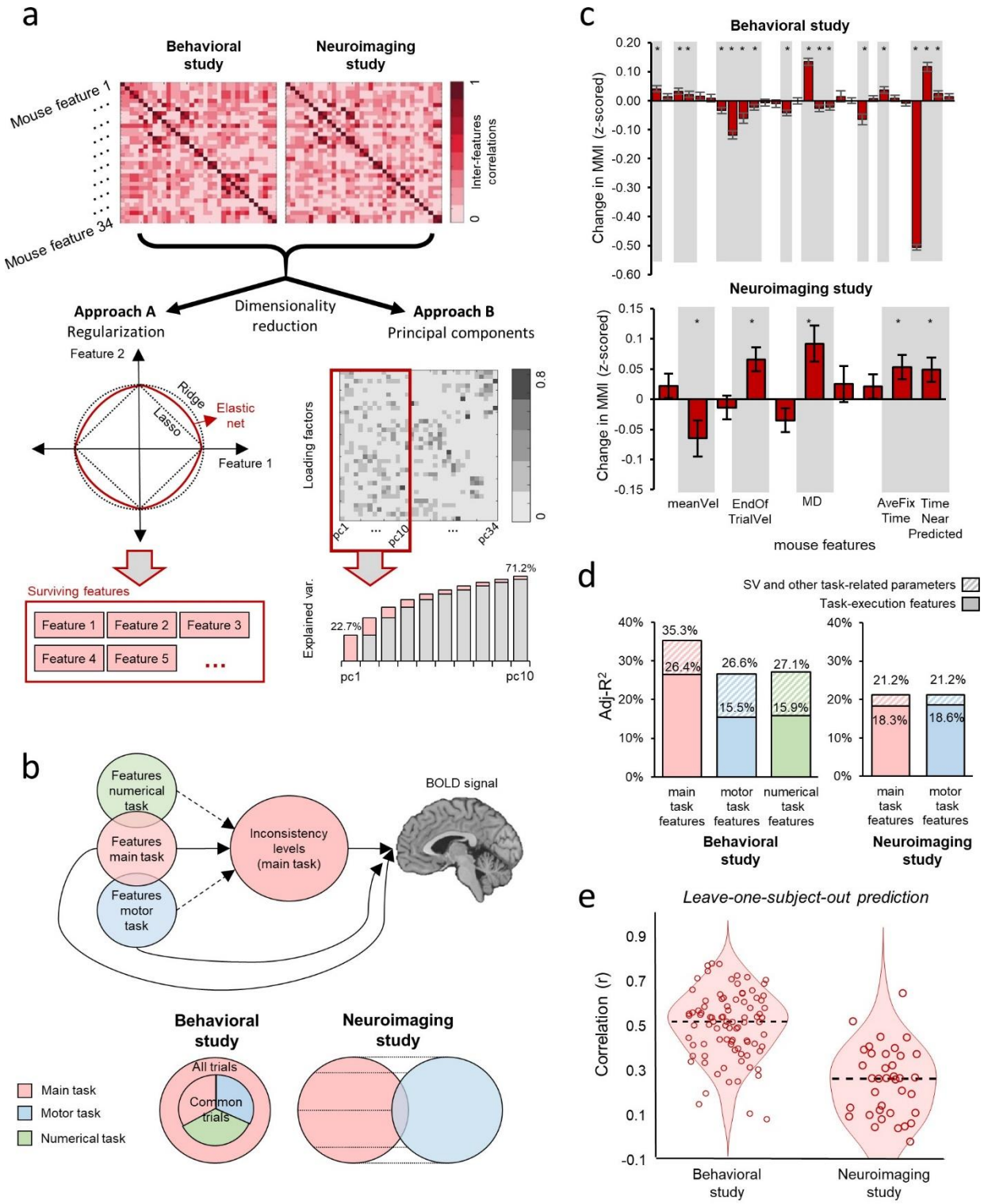

Fig. 4 | Mouse features and inconsistency levels. (a-b) Analysis strategy. (a) We took two dimensionality reduction approaches, in each of the studies, due to high dimensionality relative to the number of trials per subject, as well as due to inter-features correlations (upper row). In 68 (behavioral study) and 45 (neuroimaging study) pairs out of the 561 off-diagonal correlations, the mean correlation coefficient was higher or equal to 0.4 in absolute value. Approach A (*left)*: elastic net, which combines two methods for regularized regression (LASSO and Ridge), and maintains interpretability of the features. See Supplementary Table 4 for the list of features, which survived the elastic net regularization. Approach B (*right*): PCA. This approach preserves all features data on the expense of interpretability. In all further analyses, we used the first 10 components, which accounted for 71.2% (behavioral study) and 78.8%

(neuroimaging study) of the variance in the data. (b) In the main value-based task, we used the selected features from Approach A and the PCs from Approach B to account for MMI scores. We then repeated the analysis in Approaches A and B with mouse features from the non-value motor tasks as out-of-sample predictors for MMI scores estimated in the value-based task. In the out-of-sample analysis, we solely used the common trials across tasks (51 trials in the behavioral study, and all 75 trials in the neuroimaging study). For the fMRI analysis, we used the selected features and looked for brain regions that correlated with both motor dynamics and MMI scores. (c) Mouse features in the main value-based task correlated with inconsistency levels in both studies (Approach A). Shaded areas indicate a significant predictor ($p<0.05$) in a subjects fixed-effects regression that also included control variables (see Methods). *Upper panel*: behavioral study. *Bottom panel:* neuroimaging study (for the list of features see Supplementary Table 4). (d) Adj-R^2 from the analyses described in (b) show that mouse features accounted for inconsistency levels in- and out-of-sample in both studies (Approach A, selected features). Solid fill indicates regressions, which only included task-execution mouse features. Striped fill indicates additional explained variance from SV and other task-related parameters (see Methods). (e) Leave-one-subject-out prediction. Distribution of correlation coefficients between predicted inconsistency levels based on the selected mouse features from the main task and actual MMI scores. *Left* - Behavioral study: median: 0.490, min=0.088, max=0.796, std=0.153. *Right* - neuroimaging study: median: 0.253, min=-0.113 max=0.627, std=0.166. Dashed black line indicates median. Scatter shows individual correlation coefficients (behavioral study: N=89, neuroimaging study: N=42). (c-e) See Supplementary Fig. 5 for the results for *Approach B: PCA*.

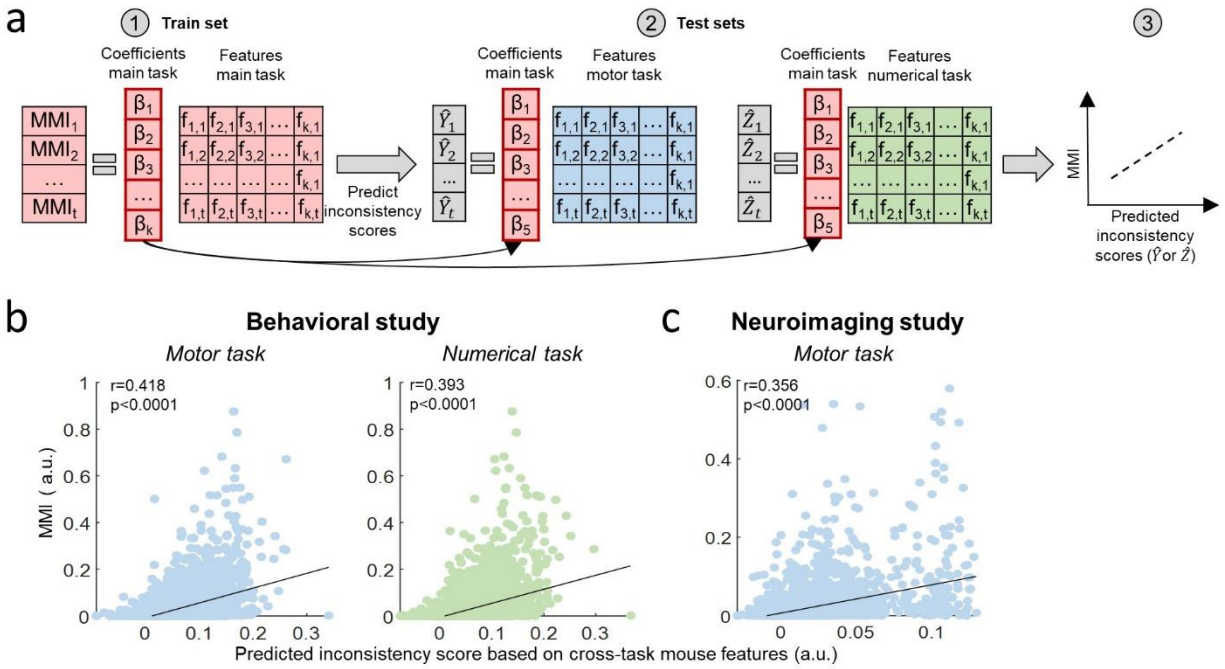

Fig. 5 | Cross-tasks prediction. (a) We use the coefficients from a regression of MMI scores on mouse features from the value-based task to predict inconsistency scores with mouse features from the non-value tasks. We then correlate predicted scored with actual MMI scores. (b-c) Obtained correlations between predicted and actual MMI. Each dot in the scatter relates to a different trial. (b) Behavioral study. *Left:* predictions based on mouse features from the motor task (N=4,306). *Right:* predictions based on mouse features from the numerical task (N=4,373). (c) Neuroimaging study (N=2,998). See supplementary Fig. 5c for the results for *Approach B: PCA*.

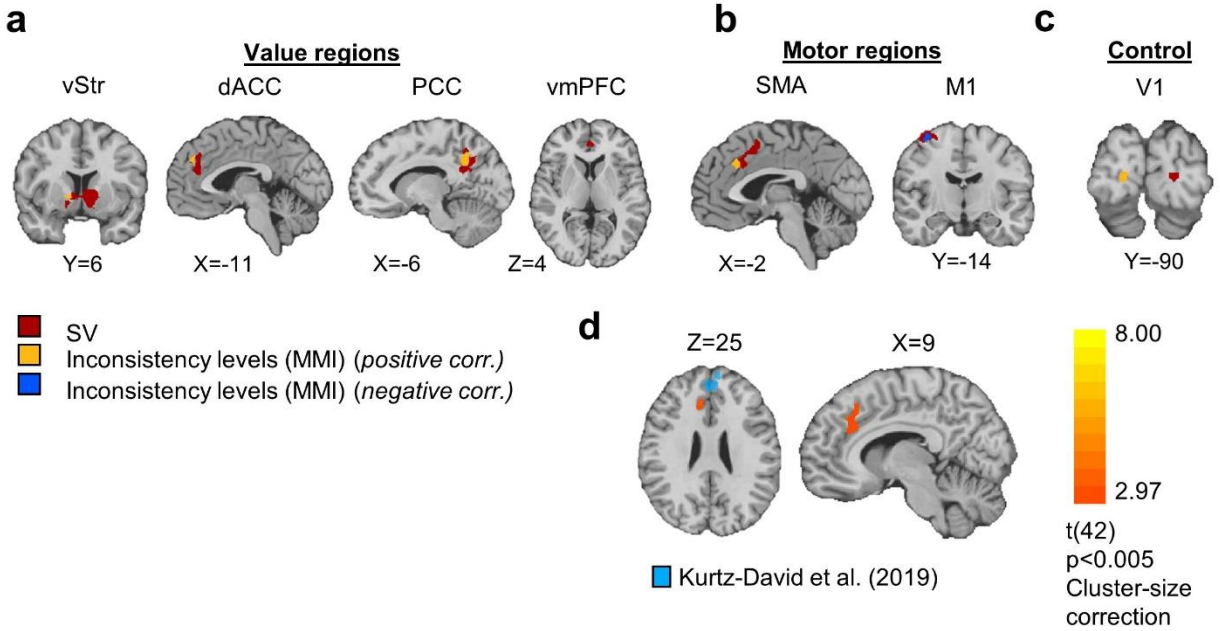

Fig. 6 | Choice inconsistency correlates with value and motor neural activations. (a-d) An overlay of the MMI and SV regressors. (ROI RFX GLM, n = 42, p<0.05, cluster-size correction. Model regression: $BOLD = \beta_0 + \beta_1 RT + \beta_2 MMI_{trial_specific} + \beta_3 SV + \beta_4 slope + \beta_5 endowment + \varepsilon$. Six additional motion-correction regressors were included as regressors of no interest. (a) Replication of the main finding in Kurtz-David et al. (2019)[18] in value-related ROIs: vStr, dACC, PCC, vmPFC. (b) motor-related brain regions: M1 and SMA. (c) Control ROI: v1. (d) A whole-brain analysis reveals inconsistency levels correlated with the same region found in Kurtz-David et al. (2019)[18] (blue). Model regression: $BOLD = \beta_0 + \beta_1 RT + \beta_2 MMI_{trial_specific} + \varepsilon$. Six additional motion-correction regressors were included as regressors of no interest. N = 42, p<0.005, cluster-size correction with 1,000 MC iterations. Results are shown on the Colin 152-MNI brain.

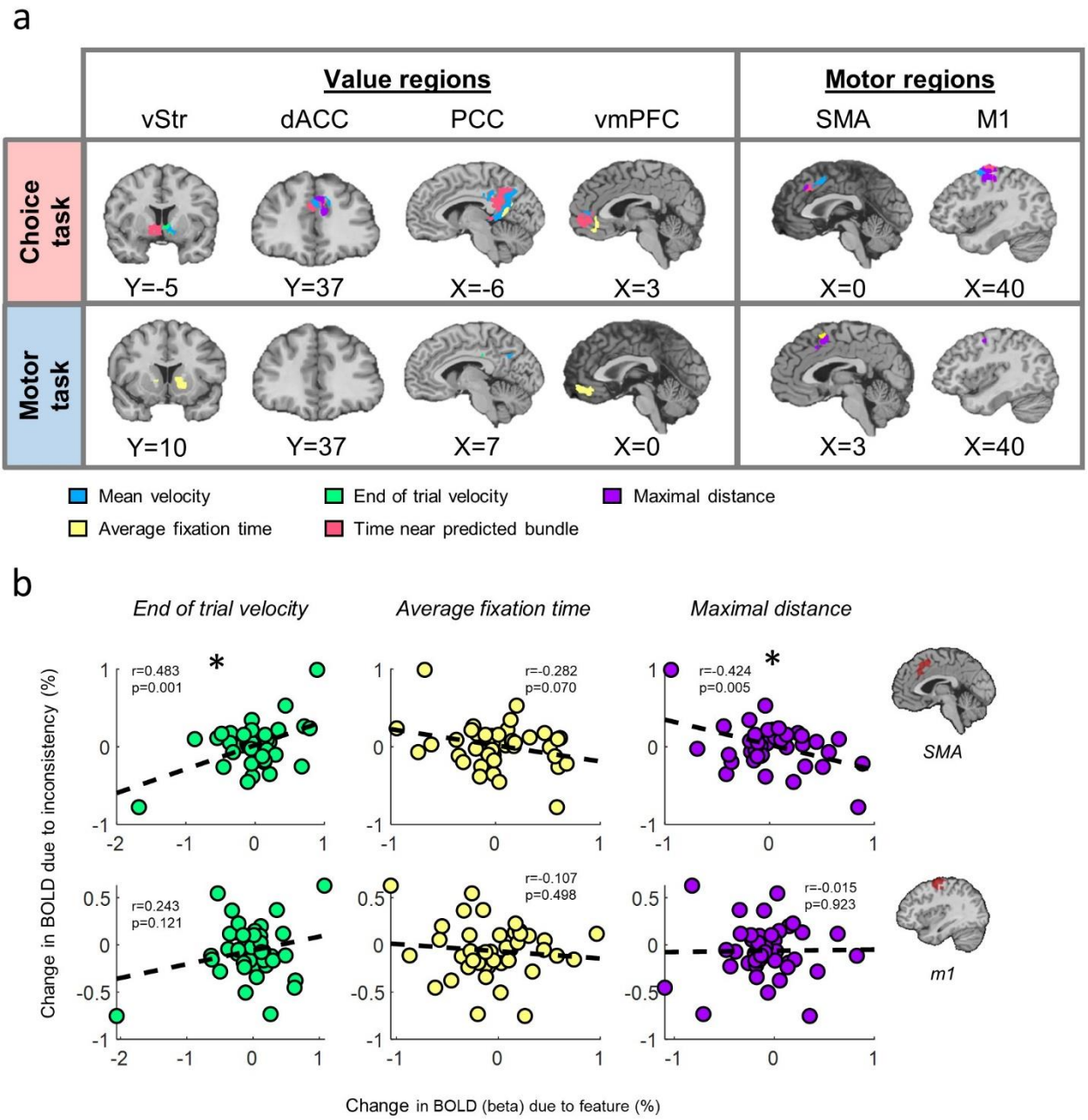

Fig. 7 | Neural correlates of motor dynamics (*elastic net based features*). (a) An overlay of the neural correlates of motor features, which were selected by the elastic net analysis. *Upper row:* main risky-choice task. *Bottom row:* motor task. Left column presents value-related ROIs, whereas the right column presents motor ROIs. ROI RFX GLM, n = 42, p<0.05, cluster-size correction. Model regression: $BOLD = \beta 0 + \beta 1\ RT + \beta 2\ meanVel + \beta 3\ EndOfTrialVel + \beta 4\ MaxDist + \beta 5\ AveFixation + \beta 6\ TimeNearPredicted + \beta 8\ slope + \beta 9\ endowmnt + \varepsilon$. Results are shown on the Colin 152-MNI brain. (b) Neural activations of mouse features in motor brain regions correlated with the neural representation of inconsistency levels. We correlated *across subjects* the change in BOLD signal (beta) attributed to a mouse feature in the RFX GLM presented in Fig. 7a (upper row), with their change in the BOLD signal (beta) attributed to MMI in the RFX GLM presented in Fig. 6b. *Up:* SMA ROI, *bottom:* m1 ROI. (*) indicates q(FDR)<0.05.

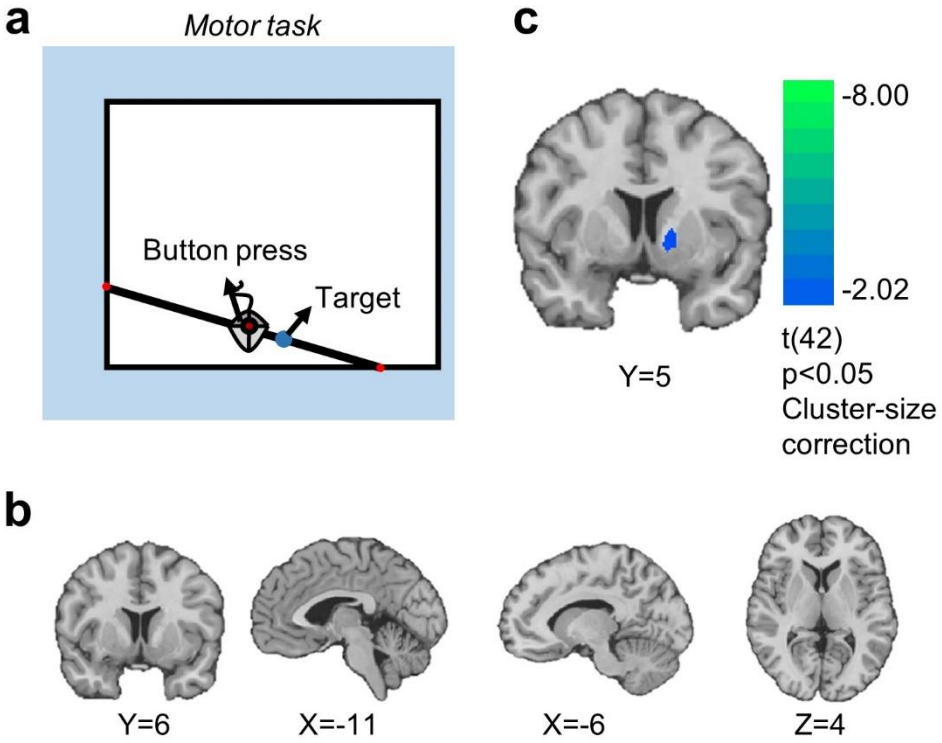

Fig. 8 | Ruling out value modulation in the motor task. (a-b) "As-if" analysis. (a) We treated the button-press location in the motor task as if it was a choice in the value-based risky-choice task. Based on this assumption, we then extracted utility-parameters, corresponding to this location, and calculated what would be its trial-specific-MMI score and trial-specific-SV had it been a lottery choice in the value-based risky-choice task. (b) We repeated the same ROI RFX GLM from Fig. 6a-c on the BOLD signal from the motor task with the "as-if" MMI and SV regressors. We looked for neural correlates of the "as-if" SV regressor, but got null results in all value-related ROIs, indicating that the motor task did not involve any sort of value modulation. (c) A reinforcement signal for reaching the target in the motor task. For each TR, we calculated the current Euclidean distance from the target. We then ran a RFX GLM in value-related regions and found that this distance was negatively correlated with vStr activation, suggesting that this region became more active when subjects were approaching the target. This indicates that in the motor task subjects did not perform a value-based decision-making, but rather determined on target-reaching. n=42, p<0.05, cluster-size correction. Model regression: $BOLD = \beta_0 + \beta_1 RT + \beta_2 EucDistance + \beta_3 slope + \beta_4 Y_Intersection + \varepsilon$. Six additional motion-correction regressors were included as regressors of no interest. Results are shown on the Colin 152-MNI brain.